

**A COMPARISON OF ELEMENTAL ABUNDANCES DERIVED FROM CHANDRAYAAN-2 CLASS AND CHANDRAYAAN-1 M<sup>3</sup> FROM THE WESTERN NEAR SIDE OF THE MOON.** M. Bhatt<sup>1</sup>, S. Narendranath<sup>2</sup>, N. Srivastava<sup>1</sup>, Netra S Pillai<sup>2</sup>, C. Wöhler<sup>3</sup>, A. Bhardwaj<sup>1</sup>, <sup>1</sup>Physical Research Laboratory, Ahmedabad, 380009, India. <sup>2</sup>U R Rao Satellite Centre, ISRO, Bengaluru, India. <sup>3</sup>Image Analysis Group, TU Dortmund University, Otto-Hahn-Str. 4, 44227 Dortmund, Germany. ([megha@prl.res.in](mailto:megha@prl.res.in)).

**Introduction:** The mapping of refractory elements is an important tool for revealing the petrological characteristics of the Moon and for understanding its geological evolution [e.g., 1, 2]. Several direct and indirect models for deriving refractory elements (Fe, Ti, Si, Al, Ca, and Mg) have been proposed over the last few decades based on the remote sensing observations of the Moon's surface in UV-VIS, NIR, X-ray and Gamma ray wavelength regions [e.g., 3-6]. Gamma-ray and X-ray spectroscopy are direct detection techniques that provide elemental maps at tens of kilometers spatial resolution [5, 6]. Optical spectroscopy techniques in the UV-VIS-NIR range is an indirect way of estimating the chemical composition of the regolith that can improve the spatial resolution to hundreds of meters [3, 4]. However, indirect techniques need a good understanding of several other factors like space weathering effects, photometric, topographic and thermal effects which have to be removed in order to successfully derive the elemental abundances.

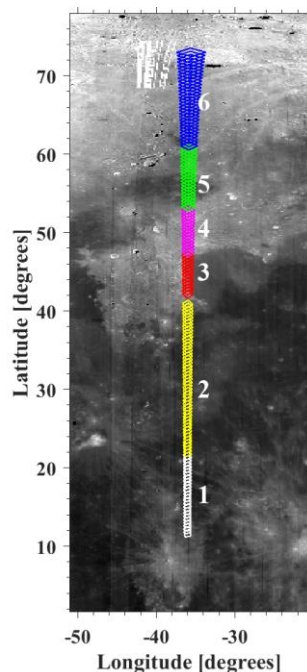


Fig. 1: M<sup>3</sup> albedo mosaic (1.5  $\mu\text{m}$ ) of the study region with the CLASS footprints overlaid. The footprints have been divided into six sections and color-coded.

In this study we compare the abundance of Al, Mg, and Si estimated using the Chandrayaan-2 Large Area Soft X-ray Spectrometer (CLASS) [7] with the elemental abundance estimation derived using the Moon Mineralogy Mapper (M<sup>3</sup>) [8] onboard Chandrayaan-1 [9]. The CLASS instrument is similar in design to C1XS [10] but with a four times larger geometric area, resulting in a spatial resolution of 12.5 km from the 100 km polar orbit of Chandrayaan-2 [11].

**Data-sets and Methods:** The M<sup>3</sup> data were processed using the framework of [12]. We resampled the level 1B 140 m/pixel M<sup>3</sup> radiance dataset [8] to a 20 pixels per degree global mosaic. The nearly global coverage of M<sup>3</sup> have been used efficiently for estimating abundances of the refractory elements Fe, Ti, Ca and Mg, where accuracies of about 1 wt.% were achieved [4, 13]. The multivariate regression model is based on global elemental maps obtained by the Lunar Prospector Gamma Ray Spectrometer (LP GRS) [14] and a several spectral parameters that are insensitive to the effects of soil maturity [4]. The CLASS observations from 18th November, 2019 [11] cover the region from the nearside equatorial (11.5N, 36W) to the northern part (72.9N, 35.5W) and observed enhanced XRF signal from lunar surface. This orbit of the CLASS instrument covers geologically diverse lithologies (Fig.1) divided into six regions of interest (ROIs). The CLASS individual footprints have been averaged corresponding to the defined ROI and named as CLASS pixel 1-6. CLASS detected the XRF lines from Mg, Al and Si in all six pixels and therefore these elements have been extracted from M<sup>3</sup> derived elemental maps for a comparison. The CLASS X-ray spectra are modeled in XSPEC using a Gaussian function for the XRF lines and converted to elemental abundances using the technique of [15].

**Results and Discussion:** The compositional diversity of the observed region and availability of comprehensive information from previous remote sensing missions [e.g., 13, 16] serve as a comparison for CLASS-derived elemental abundances. Fig. 2 shows the averaged soil reflectance and continuum-removed spectra from the ROIs shown in Fig. 1. The representative M<sup>3</sup> reflectance spectra corresponding to the CLASS averaged pixels display both band I and band II with different values of band area and centre wavelength, indicating compositionally different basal-

tic flows (Fig. 2). In Mare Imbrium (pixel 2), the high-titanium basalt, also considered as one of the iron-richest region on the Moon with FeO abundances of 22-25 wt.% [4, 5], is characterized by a broad 2- $\mu$ m band and a deeper 1- $\mu$ m band (Fig. 2). Basalts from Mare Frigoris (pixel 5) have higher MgO and Al<sub>2</sub>O<sub>3</sub> [4] compared to Mare Imbrium and are categorized by a similar 1- $\mu$ m absorption band depth as Mare Imbrium but with no or a weak 2- $\mu$ m absorption band. The feldspathic highlands (pixel 6) and the region between Mare Imbrium and Mare Frigoris (pixel 4) are characterized by higher reflectance and weak absorption bands. The CLASS footprints samples the ray systems of the craters Kepler, Aristarchus and Copernicus (pixel 1). The 1- $\mu$ m band centre position of the representative spectrum corresponding to CLASS pixel 3 is shifted to lower wavelengths, indicating a compositionally different basalt in comparison to Mare Imbrium and Mare Frigoris.

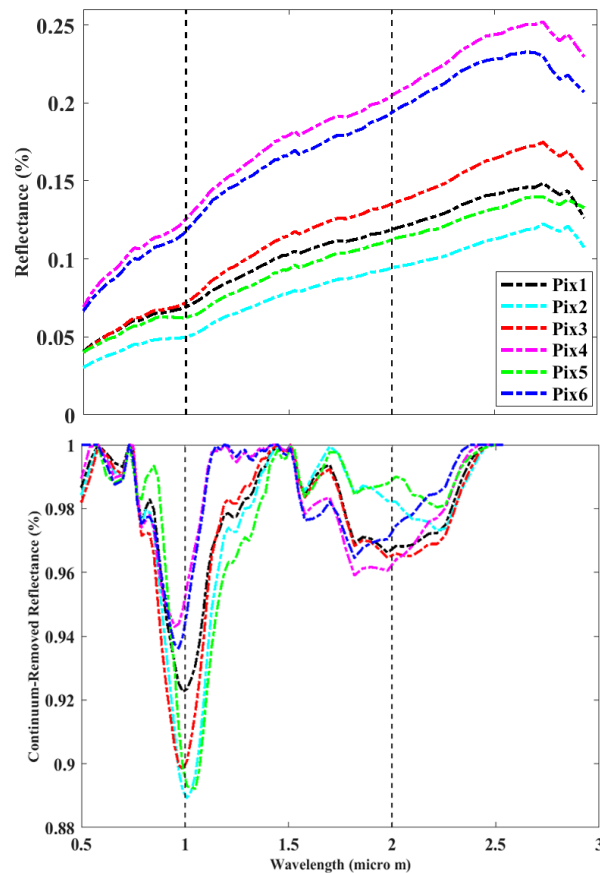


Fig. 2: The averaged M<sup>3</sup> soil spectra extracted corresponding to sections in Fig. 1. The averaged spectra are shown at the top and the corresponding continuum-removed spectra at the bottom.

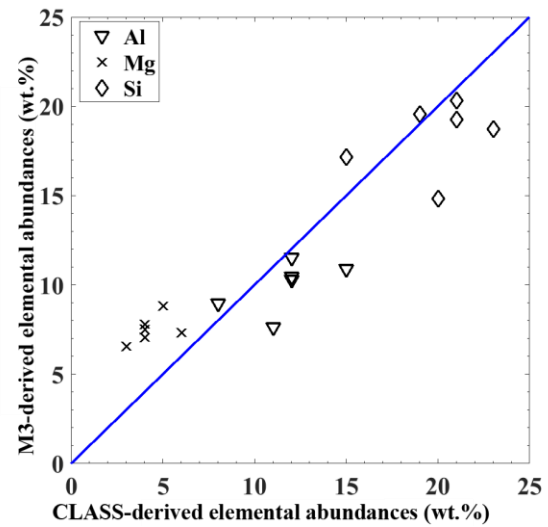


Fig. 3: Comparison of elemental abundances derived from CLASS and from M<sup>3</sup>. The RMSE is about 3 wt.%.

Fig. 3 presents a comparison between the CLASS-derived and the M<sup>3</sup>-derived Al, Mg and Si abundances of the regions corresponding to the six CLASS pixels. It shows similar trends with RMSE values of 2-3 wt.%.

**Conclusion:** This work describes our first attempt of comparing the CLASS and M<sup>3</sup> derived elemental abundances. The derived elemental abundance trends are comparable but the absolute values differ by about 2-3 wt.%. This approach will be extended to CLASS observations obtained during strong solar flares, enabling us to compare Fe, Ti and Ca which play a major role in distinguishing compositionally different basalts.

**Acknowledgements:** We downloaded the M<sup>3</sup> and LP datasets from the public domain. Our sincere thanks go to the Chandrayaan-2 mission teams.

**References:** [1] Warren, P.H. (1985) *Ann. Rev. Earth Planet. Sci.* 13, 201–240. [2] Neal, C. R. (2009) *Geochemistry* 69, 3-43. [3] Hapke, B. et al. (2019) *Icarus* 321, 141-147. [4] Bhatt, M. et al. (2019) *A&A* 627, A155. [5] Lawrence, D. J. et al. (1998) *Science* 281,1484-1489. [6] Crawford, I. A. et al. (2009) *Planet. Space Sci.* 57, 725-734. [7] Radhakrishna et al. (2011), 42nd LPSC abs.1708. [8] Pieters, C. et al. (2009) *Current Science* 96, 500-505. [9] Goswami, J. and Annadurai, M. (2009) *Current Science* 96, 486-491. [10] Grande et al. (2009) *PSS*, 57,717. [11] Narendranath, S. et al. (2020) 51<sup>st</sup> LPSC (this year). [12] Wöhler, C. et al. (2017) *Science Advances* 3, e1701286. [13] Bhatt, M. et al. (2015) *Icarus* 248,72-88. [14] Prettyman et al. (2006) *JGR* 111, E12007 [15] Athiray et al (2013) *PSS* 75, 188. [16] Varatharajan et al. (2014) *Icarus*, 236, 56-71.